

# Resolving power: A general approach to compare the discriminating capacity of threshold-free evaluation metrics

Colin S. Beam\*

Last revised: March 2023

## Abstract

This paper introduces the concept of *resolving power* to describe the capacity of an evaluation metric to discriminate between models of similar quality. This capacity depends on two attributes: 1. The metric’s response to improvements in model quality (its signal), and 2. The metric’s sampling variability (its noise). The paper defines resolving power as a metric’s sampling uncertainty scaled by its signal. Resolving power’s primary application is to compare the discriminating capacity of threshold-free evaluation metrics, such as the area under the receiver operating characteristic curve (AUROC) and the area under the precision-recall curve (AUPRC). A simulation study compares the AUROC and the AUPRC in a variety of contexts. The analysis suggests that the AUROC generally has greater resolving power, but that the AUPRC is superior in some conditions, such as those where high-quality models are applied to low prevalence outcomes. The paper concludes by proposing an empirical method to estimate resolving power that can be applied to any dataset and any initial classification model.

## 1. Introduction

A large and growing collection of metrics are used to evaluate binary classification models. Model evaluation serves a variety of functions (Raschka 2018). One is to provide a good description, meaning that the metric is sensitive to aspects of quality that are relevant to the user. Simple classification accuracy, for example, can be misleading if there is a large skew in the class distribution where one class occurs much more frequently than the other. Evaluation is also used to select the best model from a collection of competitors. This includes selection between different model classes, such as between a simple baseline model and more complex machine learning models. And it includes selection within a model class, as occurs with hyperparameter search during model tuning. Another function of evaluation is to estimate how well a given model will perform on future, unseen cases (Saito and Rehmsmeier 2015). Metric sampling uncertainty impacts all aspects of evaluation, though is especially important for model selection.

The Receiver Operator Characteristic (ROC) curve has become a favored evaluation method for binary classification models, in part due to the shortcomings of simple classification accuracy (Fawcett 2006). More recently, many have argued that the precision-recall curve (PRC) is preferable when there is a strong class imbalance and where there is low value in true-negative predictions (Boyd, Eng, and Page 2013; Saito and Rehmsmeier 2015; Davis and Goadrich 2006). Relative to the ROC curve, the PRC gives more weight to the highest-ranked cases located in the “early retrieval area” of ROC space. These cases are especially important when capacity to act is limited, such as when a health system has resources to intervene on only their sickest patients.

Sampling uncertainty is a neglected aspect of model evaluation within the field of machine learning, (Vabalas et al. 2019) but it is essential to account for when data is limited (Boyd, Eng, and Page 2013; Dietterich 1998). There has been scant research that compares the sampling precision of PRC and ROC curves. One exception is found in Zhou (2023), who used a link prediction task on a toy network model with a tunable noise parameter. For this network model problem Zhou concludes that the AUROC and AUPRC are much

---

\*Ursa Health, cbeam@ursahealth.com

more discriminating than balanced precision, and that the AUROC is slightly more discriminating than AUPRC.

This paper seeks a general approach for comparing the discriminating capacity of evaluation metrics. At the same time, it seeks specific conclusions about when and by how much some metrics are better than others. This project is conceptually difficult since evaluation metrics themselves are used to measure quality, each encoding different assumptions about what makes a model better or worse. The paper’s strategy is to use a collection of sampling models to construct a quality dimension that serves as the common standard by which to compare evaluation metrics. The sampling models are used to assess how an evaluation metric responds to changes in model quality (its signal) and how much variability it has at a given level of quality (its noise). These two quantities are combined to form an evaluation metric’s *resolving power*, which is a type of signal-to-noise ratio. The resolving power of a microscope is its capacity to distinguish between two close objects. By analogy, the resolving power of an evaluation metric describes how well it discriminates between models of similar quality. More specifically, resolving power is defined as a metric’s sampling uncertainty mapped to a common scale.

The resolving power approach draws inspiration from Mazzanti (2020), who compares how the AUROC and the AUPRC respond to improvements in classifier quality. Mazzanti’s analysis is concerned with each metric’s adequacy as a description of performance, so does not consider the issue of sampling variability. It is also limited to just one specific mechanism for model improvement. This paper provides a more general account and considers how conclusions may change under various sequences of improving classifiers. The remainder of the paper presents the resolving power methodology and then applies it to compare the AUROC with the AUPRC.

## 2. ROC and PR curves

Our interest is in classification models that map cases to predicted classes. A *discrete* classifier is one that only outputs a class label. Applying a discrete classifier to test data produces a 2x2 confusion matrix, with rows corresponding to the predicted class and columns giving the true class. A *scoring* classifier outputs a number on a continuous scale, such as an estimated probability, that represents the degree to which a case belongs to a class (Fawcett 2006). A scoring classifier can be used to construct a discrete classifier by adopting a decision threshold.

Table 1: An example confusion matrix

	actual +	actual -
predicted +	TP	FP
predicted -	FN	TN
total	P	N

A variety of familiar evaluation metrics may be calculated for discrete classifiers, such as accuracy, recall (hit rate, sensitivity, true positive rate), precision (positive predicted value), specificity, and the F1-score. These are known as single-threshold (or threshold-dependent) metrics since they depend on choosing a specific decision threshold. In contrast, threshold-free metrics use the full range of the original scores. Examples of threshold-free metrics include the AUROC, the AUPRC, the area under the precision-recall-gain curve (AUPRG), and the Brier score, among others. Threshold-free metrics are advantageous for multi-objective optimization since they allow users to adapt the model to a specific context (Flach and Kull 2015). The AUROC and AUPRC are preferred metrics when the primary goal is to achieve good discrimination so that cases are efficiently sorted into the positive and negative classes.

The ROC curve depicts the tradeoff between the true positive rate (tpr) on the y-axis and the false positive rate (fpr) on the x-axis. A discrete classifier only gives a single point in ROC space, corresponding to its one confusion matrix. A scoring classifier gives points for every possible confusion matrix that can be formed by varying the decision threshold. The empirical ROC curve interpolates between these points to create a step

function. And as the number of points approaches infinity, the empirical curve approaches the population ROC curve.

If a decision threshold is selected to flag 50 percent of all cases and the classifier is no better than random guessing then we expect it to identify half of the positives and half of the negatives, yielding the point  $(0.5, 0.5)$  in ROC space. Similarly, a random classifier flagging 20 percent of cases is expected to have a recall of 20 percent and a false positive rate of 20 percent. The random guessing classifier, then, is given by the  $y = x$  line in ROC space. A perfect classifier ranks all positive cases above all negative cases, so it corresponds to the step function from  $(0, 0)$  to  $(0, 1)$  for all the positives, and then from  $(0, 1)$  to  $(1, 1)$  for all the negatives. Classifiers that lie above the identity line but below the perfect step function represent intermediate performance with better classifiers containing points closer to the  $(0, 1)$  northwest corner of ROC space.

The AUROC summarizes a classifier’s performance across all decision thresholds and is found by integrating the ROC curve over the  $[0, 1]$  range of false positive rates. Larger AUROC values are better, with the random classifier giving an  $\text{AUROC} = 0.5$  and the perfect classifier giving an  $\text{AUROC} = 1$ . The AUROC, as a scalar value, is especially relevant for model tuning and selection. A disadvantage of the AUROC is that it can conceal local differences in performance (Fawcett 2006). For instance, one classifier may be better for highly ranked cases while another is better for those in the intermediate or lower ranks. An important statistical property of the AUROC is that it is equal to the probability that a classifier will rank a randomly chosen positive case higher than a randomly chosen negative case (Green and Swets 1966; Hanley and McNeil 1982).

Precision-recall (PR) graphs plot precision on the y-axis and recall on the x-axis. On the PR graph a random classifier corresponds to the horizontal line  $y = \frac{P}{P+N}$  = prevalence where  $P$  is the number of positive cases and  $N$  is the number of negative cases. PR curves are sensitive to class skew while ROC curves are not. This is because inputs to the ROC curve, the true and false positive rates, only depend on the column sums of the confusion matrix. Precision depends on the row sum of true and false positives so, all else equal, it will decrease with decreasing prevalence. Insensitivity to skew has been described as both an advantage (Fawcett 2006) and disadvantage (Saito and Rehmsmeier 2015) of the ROC curve.

Just like the AUROC, the AUPRC reduces a scoring classifier’s performance to a single value, with larger values indicating better performance. The AUPRC may also be interpreted as a probability, namely as the classifier’s “average precision” over the  $[0, 1]$  range of recall values. There is a one-to-one correspondence between empirical ROC and PR curves since they both chart a unique mapping from confusion matrices to points in ROC or PR space (Davis and Goadrich 2006). Davis and Goadrich (2006) show that the AUROC and AUPRC give the same model rankings when one curve “dominates” another. Informally, one curve dominates another if it lies above or equal to it across their domains. A dominating ROC curve will be northwest of the dominated curve, where its tpr is higher, its fpr is lower, or both. And a dominating PR curve will be northeast of a dominated curve, with higher precision, recall, or both across the entire domain. When there is no domination (when two curves cross) the AUROC and AUPRC can give different rankings. In cases of disagreement the AUPRC favors classifiers with better performance in the early retrieval area, which is the region of low false positive rates in ROC space.

Because it gives more weight to the early retrieval area, the precision-recall curve is often recommended for highly-skewed datasets. Yet the empirical PRC is an imprecise estimate of the true curve, especially for data with small sample sizes and strong class imbalance (Brodersen et al. 2010). This raises the question of whether the advantages of the PRC are worth its cost in precision. To answer this question we must be able to compare metrics measured on different scales.

### 3. Mapping between metrics

ROC analysis was initially developed to evaluate electronic sensors, such as radar, during World War II. In the 1950s research psychologists elaborated ROC analysis under the rubric of signal detection theory (SDT), which soon became influential within experimental psychology, psychophysics, and cognitive neuroscience (Wixted 2020). Fundamental to SDT is the specification of two probability distributions: A noise distribution for trials when the signal is absent and a signal distribution for trials when the signal is present (Green and Swets 1966). The binormal model (two Gaussians) is the most common choice for the signal and noise

distributions. The SDT framework can be described in the language of binary classification with signal present and signal absent trials considered members of the positive and negative classes, respectively.

A classification model applied to feature measurements generates class score distributions. For a simple example, suppose the two classes are adult women and men and that there is one feature (predictor) of height. The classification model will just be the identity mapping applied to the height measurements. The binormal model should then be a good approximation for the score distributions.<sup>1</sup> Figure 1 shows the binormal model for this example, using height distribution parameters from Our World in Data (Roser, Appel, and Ritchie 2013). Women have an average height of 164.7 cm with a standard deviation of 7.1 while men have an average height and standard deviation of 178.4 cm and 7.6 cm, respectively. The vertical dashed line is an example of a decision threshold, where any person above 171 cm is classified as a man and any below as a woman (this type of rule might be used in low visibility contexts where height is the most salient feature). Hit rates and false alarm rates can be calculated for that decision threshold, giving one point in ROC space.

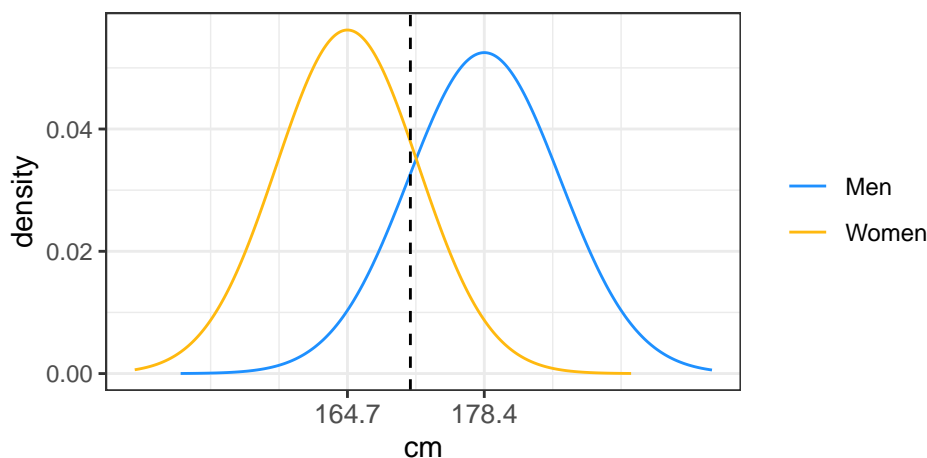


Figure 1: A binormal classifier example. The distribution of men’s and women’s heights approximately follow a normal distribution. The model implies an AUROC of .906. The vertical dashed line at 171 cm is an example decision threshold.

The amount of overlap in the class score distributions indicates the quality of a classification model. Perfect classifiers have no overlap between class scores while totally overlapping distributions indicate a random classifier. A classification model hypothetically applied to an entire population of feature measurements will give population class score distributions. These distributions, in turn, imply a population ROC curve and its AUROC value. For the binormal model there is an analytic expression for the AUROC as a function of the means and variances of the score distributions (Marzban 2004). The binormal model parameters shown in Figure 1 imply an  $AUROC = 0.906$ . Recall that this means that there is about a 90 percent chance that a randomly selected man will be taller than a randomly selected woman. In contrast to the AUROC, the AUPRC is a function of both the class score distributions and the outcome prevalence. Brodersen et al. (2010) show how to approximate the AUPRC for a given binormal model using numerical integration.

Classifier improvement, such as occurs during model tuning, can be represented as a process that diminishes the overlap in the class score distributions. An ordered sequence of increasingly separated distributions constructs a quality dimension that can be used to unify disparate metrics. For each set of score distributions in the sequence we can find the associated pairs of AUROC and AUPRC values, tracing out a curve in the  $AUROC \times AUPRC$  plane. This curve forms a mapping that we will use to compare the AUROC and the AUPRC.

The primary challenge of this strategy is that the mapping between metrics depends on how the score

<sup>1</sup>Height is believed to result from the sum of a large number of independent genetic and environmental effects. So by The Central Limit Theorem, the height distribution should be approximately normal.

distributions are ordered. There are myriad ways to increase separation between distributions, with each way indicative of different types of improvement. Beginning with a binormal model, we can manipulate separation by adjusting the means or variances and still retain a binormal model. One simple approach, used below, is to add fixed increments to the positive class scores. But a concern is that this may poorly approximate how improvement happens in practice. This paper solves this ambiguity by fiat: It assumes that simple manipulations of score distributions are a reasonable description of model improvement. Nonetheless, one can still test the importance of this assumption by specifying alternative distribution sequences and then assessing their impact.

We have identified the quality dimension as an ordered sequence of distributions, but how should we measure location on this dimension? One option is to just use the model rankings themselves, which will form an ordinal scale (Stevens 1946). Another option is to measure distribution overlap directly using the Bhattacharyya coefficient. Or we can use a measure that relates overlap to model quality, the AUROC and AUPRC being two examples among many. The AUROC has several properties that make it a good choice. Since the AUROC is an area (and a probability), equal differences across the scale represent equal differences in amount. Another advantage, mentioned above, is that it is unaffected by outcome prevalence. The AUROC is also the most popular threshold-free evaluation metric for binary classifiers, making it a natural choice as the standard reference metric.

For our purposes, the AUROC’s biggest advantage is that it is agnostic with respect to where changes occur in the score distributions. This fact is easiest to demonstrate with an empirical score distribution, defined as a finite set of risk scores and associated outcomes. Briefly, suppose there are  $n^+$  positive cases,  $n^-$  negative cases, and that all risk scores are unique. Further suppose that the classifier is not perfect, so  $0.5 \leq \text{AUROC} < 1$ , and we want to improve this by perturbing the risk scores. If we sort all the cases together into a single list ranked by score, then the smallest improvements occur by finding pairs of adjacent risk scores that are “out-of-order,” such that the negative case has a higher score than the positive case, and re-ordering these pairs. Re-ordering a single pair will improve the AUROC by  $\frac{1}{n^+} \times \frac{1}{n^-}$  regardless of where the improvement occurs. This follows from the Riemann sum method of AUROC estimation: resolving any pair of adjacent scores will add a rectangle with base  $\frac{1}{n^-}$  and height  $\frac{1}{n^+}$  to the area under the ROC curve. In contrast, the AUPRC will improve more for resolving out-of-order pairs that are among the highest-ranked risk scores.

To summarize this section’s key points: Classifier quality is gauged by its outputs, the class score distributions. A sequence of increasingly separated class distributions forms a common quality dimension that charts the relationship between different evaluation metrics. A key caveat is that the mapping between metrics is contingent on how the score distributions are separated. Characteristics of the AUROC make it a good choice as the reference measure of model quality. In particular, the AUROC always improves by a constant amount when resolving a pair of out-of-order risk scores.

## 4. Resolving power

The resolving power method can be summarized in four steps:

1. **Sampling model:** Specify the class score distributions, prevalence, and sample size.
2. **Response curves:** Use the sampling model to create a fine grid of improving classifiers. Find each metric’s values across the grid.
3. **Random sampling:** Estimate metric sampling uncertainty by drawing random samples from points of interest within the quality grid.
4. **Comparison:** Use the results of steps 2 and 3 to estimate and compare resolving power.

This section illustrates the core mechanics of the approach using an idealized example while later sections move to the applications. Suppose we are interested in comparing the resolving power of the AUROC with that of the “area under the super-great curve” (the AUSGC). We construct a sampling model by specifying the class score distributions, prevalence, and sample size. Next, we create a grid of 1000 models. The first model has totally overlapping distributions for the random classifier and then we gradually shift the distributions apart so that the 1000th model has almost no overlap. Finally, we want to assess sampling

models that give AUROC values of 0.7 and 0.9. We draw many replicates from these two models to estimate the sampling variability of the two metrics. Results of the analysis are summarized in Figure 2 below.

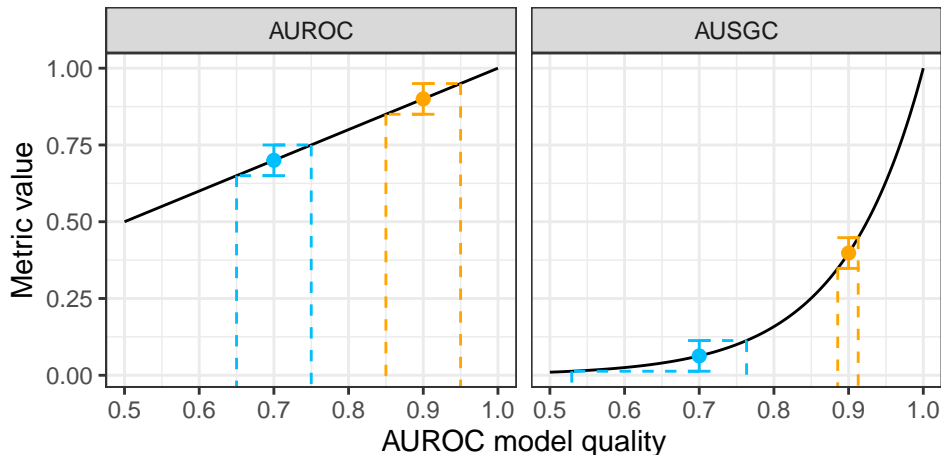


Figure 2: Response curve example. The two panels are united by the same sequence of models used to construct the quality grid. The AUROC serves as the common reference scale on the x-axis.

Following the previous section’s recommendation, the AUROC on the x-axis serves as the reference scale for quality. The left panel, then, just gives the identity mapping. The right panel shows how the AUSGC changes relative to the AUROC, giving the relative signal of the two metrics across the quality continuum. Unit slope indicates equal signal, a slope less than one favors the AUROC, and a slope greater than one favors the AUSGC. For a given point on the curve repeated draws from the sampling model will estimate each metric’s noise distribution. Response curves then allow us to map each metric’s uncertainty interval to a model quality interval, which forms the common basis for comparison.

Previously we defined resolving power generically as a metric’s scaled sampling uncertainty, but now we need to make this specific. Define a metric’s *resolution* as the width of its 95 percent confidence interval mapped to the quality scale. We will denote metric resolution with the Greek letter  $\kappa$ . A microscope’s resolution limit is the smallest distance between two points that can still be distinguished as separate entities. Analogously,  $\kappa$  is the minimum distance for statistical discrimination using the  $\alpha = .05$  convention from statistical hypothesis testing. Resolving power is  $1/\kappa$ , or just the reciprocal of the resolution distance. With AUROC as the reference scale we can form the following heuristic assessments: A resolving power of 10 is rather poor, a resolving power of 100 is decent, and a resolving power of 1000 is good. Of course, these assessments will depend on the context. A resolving power of 100 is much less impressive for a sample size of one million than for a sample size of ten thousand.

A disadvantage of the resolving power definition is that it requires on choosing an arbitrary  $\alpha$  level. Appendix A describes an alternative approach that expresses resolving power as a scaled standard error, thus eliminating this requirement. This comes at a cost of stronger assumptions: The alternate approach assumes that the response curve is well-approximated by a straight line and that the evaluation metric’s sampling distribution is roughly symmetric.

Returning to the example, for the AUROC 0.7 model shown in blue, we have:

- An AUROC of .7 with a 95% confidence interval of [.65, .75].
- An AUSGC of .063 with a 95% confidence interval of [.013, .114]. This maps to an AUROC quality interval of [.53, .76].

The vertical dashed lines in Figure 2 show how the response curves map the confidence limits to a common quality scale. This is trivial for the AUROC since it is the identity mapping, but is included to make clear the mechanics of the method. For the AUROC = 0.7 sampling model we can conclude that the AUSGC

is much less precise with  $\kappa_{\text{SGC}} = .23$  compared to  $\kappa_{\text{ROC}} = .1$ . Turning to the 0.9 AUROC model shown in orange, we have:

- An AUROC of .9 with a 95% confidence interval of [.85, .95]
- An AUSGC of .4 with a 95% confidence interval of [.35, .45]. This maps to an AUROC quality interval of [.89, .91].

Note that the confidence intervals in the original metrics have stayed the same width at .1 for both the AUROC and the AUSGC. However, the AUSGC is now in a steeper region of the curve, so its signal-to-noise ratio has improved. As a result, we obtain  $\kappa_{\text{SGC}} = .02$ , giving the AUSGC much better model resolution than the AUROC. From this analysis we can conclude that the AUSGC is only “super-great” when the search space spans a region of high-quality models.

## 5. Binormal model

The binormal model, as the most commonly used model in ROC analysis, serves as a good initial application of the resolving power approach. All code and simulation data used in the paper is available on GitHub.<sup>2</sup> We now apply the four steps of resolving power.

**Step 1: The sampling model.** Assume a binormal model where negative class scores have a standard normal  $\mathcal{N}(0, 1)$  distribution and positive class scores have  $\mathcal{N}(\delta_i, 1)$  distributions. The analysis explores a range of prevalence comprising the values [.01, .05, .10, .20, .30, .40, .50], which is the same set used by Mazzanti (2020). We explore a moderately sized classification task of 10,000 instances. So the lowest prevalence condition has 100 instances in the positive class.

**Step 2: Response curves.** We create a fine grid of improving models by increasing the distance  $\delta_i$  between distributions. The grid begins with the random classifier AUROC = .5 and ranges to a max AUROC = .99995. Each  $\delta_i$  is chosen to create .00005 AUROC increments between grid points. Since we have fixed three of the four binormal model parameters, we can find the shift parameter as a function of the target AUROC value (see Marzban (2004) for details). For our model it is:

$$\delta_i = \sqrt{2} \times \Phi^{-1}(\text{AUROC}) \quad (1)$$

where  $\Phi^{-1}$  is the inverse cumulative standard normal distribution and  $\delta_i$  is the shift parameter for each grid point. Note that an evenly spaced AUROC grid will require progressively larger shifts between class distributions as model quality increases. Next, we need to find the AUPRC values associated with each AUROC grid point. The AUPRC can be found from a binormal model via numerical approximation. Let  $\alpha$  represent the outcome prevalence and  $\Phi_+$  and  $\Phi_-$  represent the cumulative Gaussian distributions for the positive and negative classes, respectively. Brodersen et al. (2010) derive the PR curve by finding precision (PPV) as a function of recall (TPR):

$$\text{PPV} = \frac{\alpha \text{TPR}}{\alpha \text{TPR} + (1 - \alpha) (1 - \Phi_- (\Phi_+^{-1}(1 - \text{TPR})))} \quad (2)$$

And to find the AUPRC they numerically approximate the integral:

$$\text{AUPRC} = \int_0^1 \text{PPV}(\text{TPR}) d\text{TPR} \quad (3)$$

To summarize the steps: First we create an evenly spaced grid of AUROC values using the implied shift parameter values from equation (1). We then use the shift values in equation (2), specifically for the  $\Phi_+$  parameterization. This gives us the PR curve so that we may use equation (3) to find the associated AUPRC value.

<sup>2</sup>[https://github.com/colinbeam/resolving\\_power](https://github.com/colinbeam/resolving_power)

**Step 3: Random sampling.** We wish to assess a range of quality values by evaluating models with AUROCs of [.65, .75, .85, .95]. In the figures below these models are respectively labeled “Poor,” “Fair,” “Good,” and “Excellent.”

Figure 3 shows the binormal response curves for each condition. The relationship between metrics becomes more curvilinear as prevalence decreases. This implies that, all else equal, the AUPRC will be relatively more discriminating among higher quality models applied within low prevalence contexts. The response curve for a prevalence of .5 is approximately a straight line with an intercept of zero and a slope of one—the identity mapping. Thus, the AUPRC and AUROC are estimating the same quantity but by using different formulas. In this condition, then, differences in resolving power will be due to differences from sampling error alone.

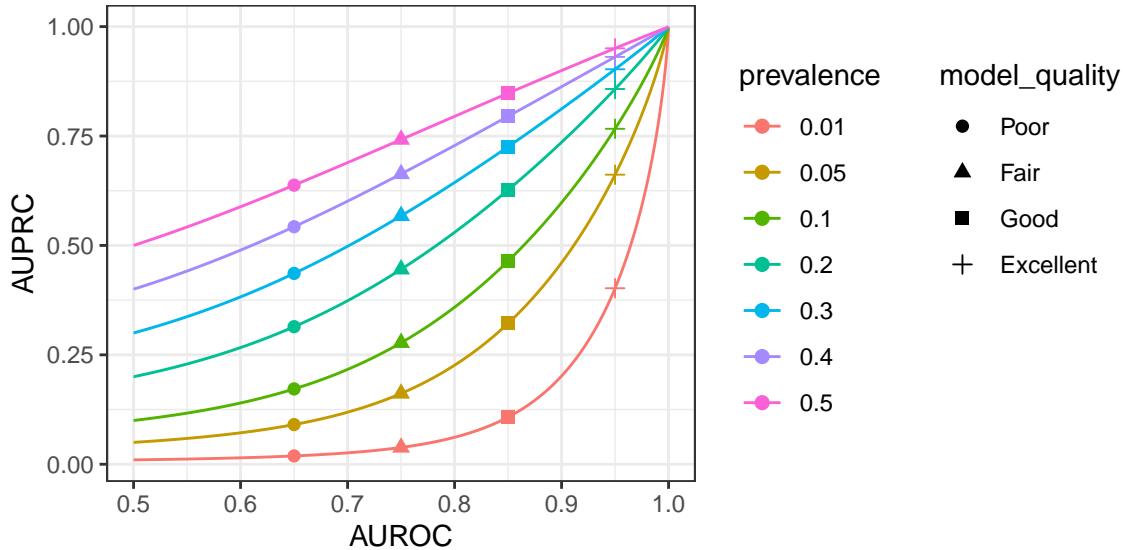


Figure 3: Mapping between AUROC and AUPRC for the binormal model.

For the four points of model quality we take 10,000 random samples from each implied binormal model and estimate AUROC and AUPRC values with the `PRROC` R package (Grau, Grosse, and Keilwagen 2015). The AUPRC is estimated using the Davis and Goadrich method (Davis and Goadrich 2006). Ninety-five percent confidence intervals are found from the .025 and .975 quantile values of the simulation samples.

**Step 4: Comparison.** For the final step we use the curves in Figure 3 to map the AUPRC 95 percent confidence interval values to the AUROC scale. We then find the relative difference in metric resolution with the AUROC as the baseline (which is equal to the relative difference in resolving power with the AUPRC as baseline):

$$\Delta = \frac{\kappa_{\text{PRC}} - \kappa_{\text{ROC}}}{\kappa_{\text{ROC}}} = \frac{1/\kappa_{\text{ROC}} - 1/\kappa_{\text{PRC}}}{1/\kappa_{\text{PRC}}}$$

To smooth out variability in the estimates the simulation was repeated three times and estimates were averaged across runs. Simulation results are shown in Figure 4.

Beginning with the prevalence = .5 “identity mapping” condition, we see that the AUPRC is usually around 10 percent more variable than the AUROC, though the disadvantage is smaller in the “Excellent” model condition. Since the grid was constructed using equal AUROC increments, an equivalent statement is that AUPRC confidence intervals contain 10 percent more models. In the remaining conditions the AUPRC suffers a greater disadvantage in the flatter portions of the response curves, corresponding to contexts of low prevalence and poor model quality. Specifically, the AUPRC is at a disadvantage for all poor (AUROC = .65), fair (AUROC = .75), and good (AUROC = .85) models across all levels of prevalence. AUPRC resolution



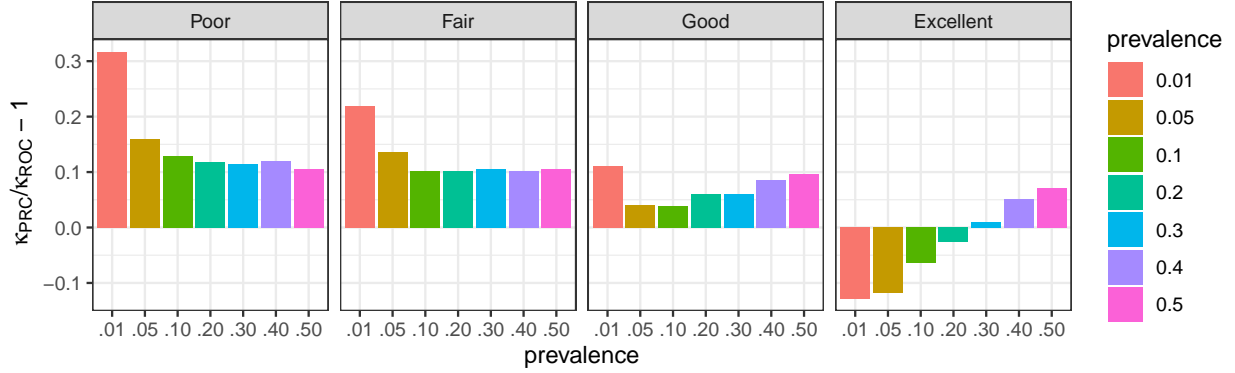


Figure 4: Relative metric resolution by outcome prevalence and model quality for a binormal model with a sample size of  $N = 10,000$ . At each level of model quality 10,000 simulations are taken from the sampling model. Confidence limits are found from the .025 and .975 quantile values of the simulation samples.

widths are typically about 10 percent larger, though in the flattest portion of the response curve—the low prevalence and low model quality condition—the disadvantage is around 30 percent. The AUPRC has better resolving power only for excellent models ( $AUROC = .95$ ) applied to moderately to strongly imbalanced datasets (prevalence of .2 and below).

Figure 4 shows relative differences, but it is also important to consider how absolute uncertainty varies across conditions. Figure 5 explores these relationships using Hanley and McNeil (1982)’s formula for the approximate standard error of the AUROC. The standard error is strongly decreasing in prevalence, shown by the separation between lines, and is especially large in the .01 condition, making relative imprecision even more costly in absolute terms. The standard error is mostly decreasing in model quality, though interestingly, slightly increases from an AUROC of 0.5 before reaching a maximum around 0.6. As an aside, the normal approximation confidence intervals using Figure 5 standard errors are typically close to the simulation confidence intervals. For a prevalence = .01 and  $AUROC = .65$  the simulation 95 percent confidence interval is [0.596, 0.702] while the normal approximation is [0.591, 0.709]. The approximation does become worse as the AUROC increases: In the prevalence = .01 and  $AUROC = .95$  condition the simulation confidence interval is [0.929, 0.967] while the normal approximation is [0.92, 0.98]. The adequacy of the normal approximation bears on the utility of the alternative method for estimating resolving power, described in Appendix A.

Thus, for moderately sized ( $N = 10,000$ ) classification tasks the AUROC will typically provide better resolution. Importantly, these results are essentially unchanged for different sample size magnitudes. For both a magnitude smaller ( $N = 1000$ ) and larger ( $N = 100,000$ ), the AUROC is generally better, with the AUPRC showing an advantage only among excellent models with an outcome prevalence of 20 percent or less. Appendix B presents results for these additional scenarios.

If risk scores follow a binormal distribution and model improvement results in additive shifts of these scores, then it will be best to use the metric with greatest resolving power for model search. Yet since these assumptions will never fully be met in practice, this section’s results should instead be received as general guidance to be weighed against other criteria, not as prescriptive. For instance, since the AUPRC suffers only a modest disadvantage for “good” models with moderate prevalence, it may still be preferable because of the greater weight it assigns to the early retrieval area.

It is uncertain how robust this section’s guidance is to deviations from the binormal model. One way to address this concern is to replace the binormal model with a domain-specific data-generating process. An example of this approach from network analysis was discussed above, where Zhou (2023) constructs networks with fixed link connection probabilities that are perturbed by additive, independent noise. This framework is amenable to a resolving power analysis—In fact, Zhou’s Figure 1 essentially displays response curves by showing how the AUROC, AUPRC and balanced precision respond to changes in the noise parameter values

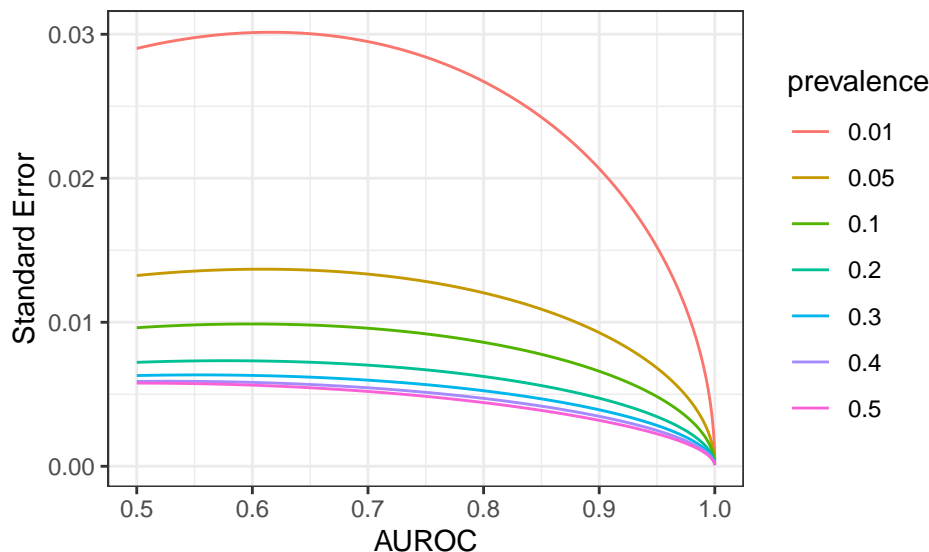


Figure 5: The relationship between AUROC and its standard error for different levels of outcome prevalence. The standard error is found using the approximation formula from Hanley and McNeil (1982).

that determine model quality.

Most applications will not be able to draw upon a quantitative framework to build domain-specific sampling models. An alternative strategy is to start with a dataset and a baseline model and then build the sampling model from an initial set of risk scores. This empirical-driven approach is explored in the next section.

## 6. Empirical sampling models

This section shows how specific problem information can be incorporated into the resolving power approach. We will explore an example task where the aim is to predict 30-day hospital readmissions among diabetes patients using features such as patient demographics, prior utilization, diagnoses, lab tests, and medications. The data for this example can be found at the UCI Machine Learning Repository.<sup>3</sup> After applying recommended restrictions, the data includes 69,973 total records with 6,277 readmissions for an outcome prevalence of about 9 percent. So this is an example of an imbalanced class problem for which the AUPRC is often recommended.

Now how might we use the data to guide our choice of a sampling model? A seemingly sensible approach is to fit an initial classifier and then use its risk scores to inform the choice. The initial model might be the simplest algorithm among a set of candidates, or it could be a preferred algorithm using its default hyperparameters. We may then construct a sampling model from the empirical distribution (the set of outcomes and risk scores) in a couple of different ways. One is to find a parametric model that gives a good approximation to the empirical distribution. Another is to treat the empirical distribution as the population, as is done in resampling methods such as bootstrapping.

For the readmissions data, we use a simple logistic regression as the initial model, estimating risk scores using 5-fold stratified cross-validation. The estimated AUROC is .646 for this initial model. By the previous section’s taxonomy, this is a “poor” model with about a 10 percent outcome prevalence. So the binormal model results suggests that we should prefer the AUROC to the AUPRC. The distribution of patient effects are shown in Figure 6, with a rug plot and density estimates on top and qqnorm plots below.

A normal approximation does not appear appropriate as both the positive and negative class have large clusters of scores in the lower tail. We could hunt for a better parametric approximation—perhaps some type

<sup>3</sup>For access and a description of the original dataset go to <https://archive.ics.uci.edu/ml/datasets/diabetes+130-us+hospitals+for+years+1999-2008>. The post-processed data can be found at the GitHub address listed above.

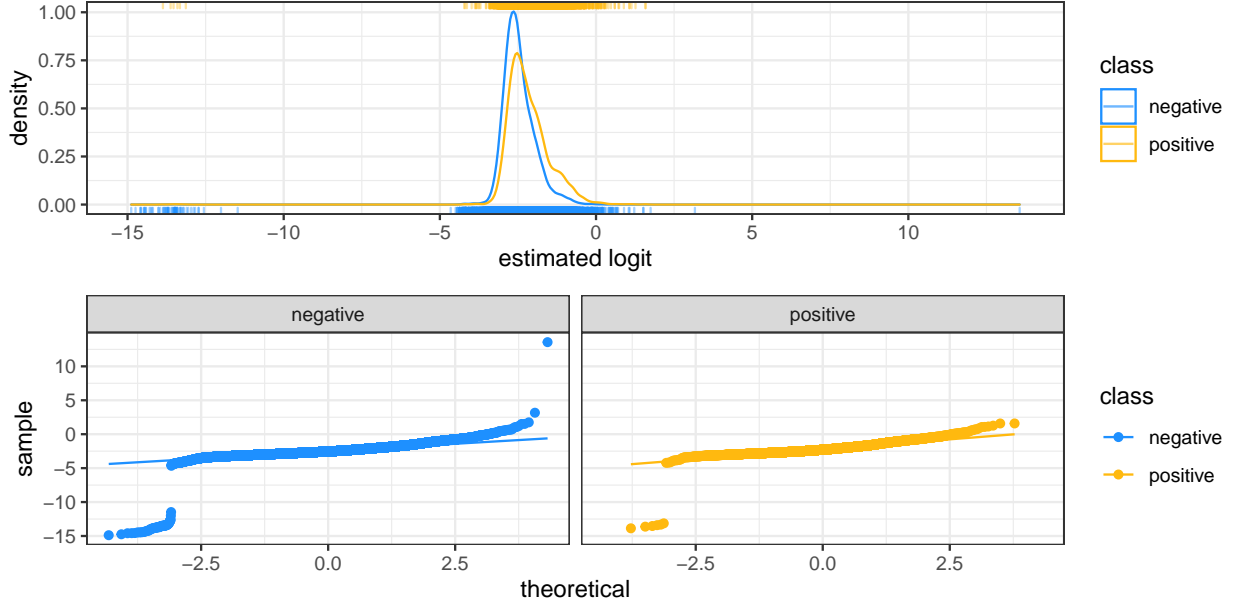


Figure 6: Top panel: Estimated logit effects with kernel density estimates for the positive and negative class. Bottom panel: Q-Q norm plots of sample versus theoretical quantiles. Straight lines pass through the 1st and 3rd quartiles.

of mixture distribution—but instead we will use the empirical distribution as the population sampling model.

Moving to the second step, how can we use an empirical sampling model to construct a response curve? A simple option is to add small increments to all positive class scores, which is analogous to the approach we used with the binormal model. Incremental improvement will then be concentrated among the negative and positive cases with the closest risk scores, wherever they may reside in the distribution. This seems reasonable as it assumes that marginally better models will first amend the ranking of cases that need the smallest adjustments.

The previous section created an evenly-spaced grid of AUROC values using binormal model analytic results. An evenly-spaced grid is also possible for an empirical distribution: To begin, suppose there are  $n^+$  positive cases with risk scores  $r_i^+$  for  $i \in \{1, \dots, n^+\}$  and  $n^-$  negative cases with risk scores  $r_j^-$  for  $j \in \{1, \dots, n^-\}$ . Further suppose all risk scores are unique and that the classifier is not perfect, so  $r_i^+ < r_j^-$  for at least one  $(i, j)$  pair. This implies that  $0.5 \leq \text{AUROC} < 1$  for the initial AUROC value. We will build the grid in the direction of improving AUROC, though it is straightforward to adapt the process for decreasing AUROC. First, find  $\delta_1 = \min(r_j^- - r_i^+ | r_j^- > r_i^+)$ , so  $\delta_1$  is the smallest positive difference in risk scores between two cases that are out-of-order such that the negative case is assigned higher risk than the positive case. Similarly, we can find  $\delta_2$  as the second smallest difference,  $\delta_3$  as the third smallest, etc. Now if we add  $\delta_1 + \epsilon$  to all positive class risk scores where  $\delta_1 < \delta_1 + \epsilon < \delta_2$  we will shift the positive distribution just enough to resolve one pair of out-of-order risk scores, but no more. Then by the Riemann sum method we know that the AUROC will improve by  $\frac{1}{n^+} \times \frac{1}{n^-}$ . The result can also be deduced from the probabilistic interpretation of the AUROC since there are  $n^+ \times n^-$  unique ordered pairs of positive and negative scores, which forms the number of events in the sample space, and so resolving one pair increases the probability by  $\frac{1}{n^+ \times n^-}$ . Now if instead we had added  $\delta_2 + \epsilon$  with  $\delta_2 < \delta_2 + \epsilon < \delta_3$  then it would have fixed two pairs of scores and the improvement would have been  $\frac{2}{n^+ \times n^-}$ . Thus, we can precisely increase or decrease the AUROC in  $\frac{1}{n^+ \times n^-}$  increments. The result is useful for determining an initial increment to shift the class scores. Achieving a fixed increment across the grid requires updating the score distance calculations after each step, but this is computationally costly and will typically be unnecessary. Instead, it is most important to choose an initial

increment that creates a high density of points across the grid range so that the response curve may be reliably estimated.

Figure 7 shows the response curve constructed from shifting the readmissions class score distributions. The starting model AUROC and AUPRC values of .646 and 0.166 are shown by the dot. The curve is built by shifting the positive class distribution above and below the starting point, using an initial increment that produces a change of .001 AUROC units. Each empirical distribution along the grid is considered the population, so the associated population AUROC and AUPRC are just the sample values. There are a total of 1000 grid points, which range from .54 to .92 in AUROC and from .12 to .50 in AUPRC. In practice, it is rare to see substantial improvement from initial performance, so these ranges cover a larger space than is expected to be observed during model search. The shape of the curve in Figure 7 is similar to the binormal response curves: For lower AUROC values the slope is relatively flat but then it increases with improving model quality.

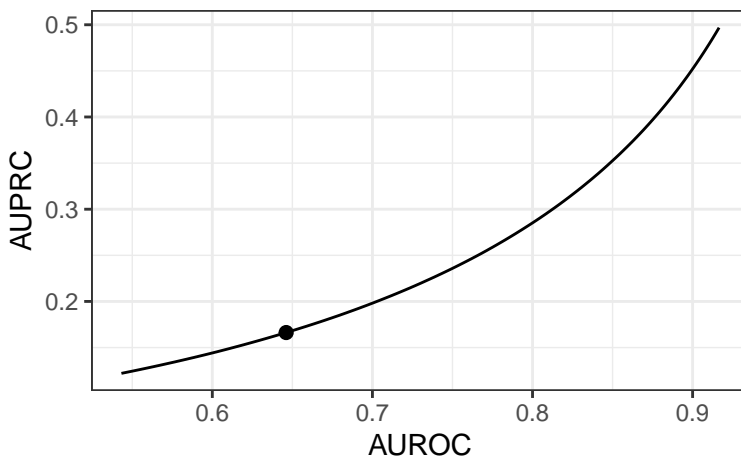


Figure 7: An empirical response curve from the readmissions data logistic regression model. The black point shows baseline performance. The curve is constructed by incrementing positive scores above and below the baseline distribution.

Moving to the third step of random sampling, the initial model is the natural choice to evaluate since improvements will be made from this starting point. We generate 10,000 samples from the empirical distribution, fixing the prevalence with stratified sampling, and then find 95 percent confidence intervals. The fourth and final step uses the response curve to estimate and compare metric resolution. Results of the sampling experiment are displayed in Table 2.

Table 2: Simulation results summary. Lower and upper CI bounds are for 95 percent confidence intervals.

<b>metric</b>	<b>Lower CI</b>	<b>Upper CI</b>	$\kappa$	<b>resolving power</b>
<b>AUROC</b>	0.6391	0.6535	0.0144	69.4
<b>AUPRC</b>	0.1601	0.1732	NA	NA
<b>AUPRC to AUROC</b>	0.6341	0.6591	0.0250	40.0

The last row uses the response curve to map AUPRC to the AUROC scale. Recall that metric resolution,  $\kappa$ , is just the width of the 95 percent confidence interval in AUROC units. The AUROC has considerably better discrimination with a resolving power that is over 70 percent greater than the AUPRC. The absolute difference in confidence interval widths is about 0.011 AUROC units, which could be substantial relative to the often small improvements achieved during hyperparameter tuning.

The robustness of these results with respect to the additive improvement assumption could be checked with a sensitivity analysis that explores other paths towards class score separation. An extreme alternative would be

to resolve errors starting with the highest risk scores first and then moving down the rankings. This would yield an immediate strong response for the AUPRC while the AUROC would be unaffected. An opposite extreme would be to improve all the lowest ranked cases first. There are also myriad intermediate strategies. One could use a mechanism similar to Mazzanti (2020), with improvements initially evenly distributed across the score distribution, but gradually becoming concentrated in the early retrieval area.

## 7. Conclusion

Resolving power allows for systematic comparison of threshold-free evaluation metrics. Central to the method is the specification of a risk score sampling model that is used to both manipulate model quality and probe sampling variability. The quality dimension, which serves as the standard for comparison, is formed as an ordered sequence of class score distributions with decreasing overlap. A response curve shows how an evaluation metric responds to changes in classifier quality (its signal). A metric's sampling variability is assessed at a point on the curve by random draws from the sampling model (its noise). The sequence of score distributions forming the quality dimension is necessarily arbitrary, so this paper elects to use simple additive shifts to increase separation. One may also conduct sensitivity analyses that test robustness to alternate sequences of distributions. Resolving power is classifier-agnostic since it operates on risk scores that are downstream of the classification model. Binormal model results provide general rules-of-thumb for when the AUROC versus the AUPRC will have relatively stronger resolving power. The empirical method allows researchers to use their data and an initial classifier of their choice to construct the sampling model used for resolving power estimation.

## References

- Boyd, Kendrick, Kevin H Eng, and C David Page. 2013. “Area Under the Precision-Recall Curve: Point Estimates and Confidence Intervals.” In *Machine Learning and Knowledge Discovery in Databases: European Conference, ECML PKDD 2013, Prague, Czech Republic, September 23-27, 2013, Proceedings, Part III 13*, 451–66. Springer.
- Brodersen, Kay Henning, Cheng Soon Ong, Klaas Enno Stephan, and Joachim M Buhmann. 2010. “The Binormal Assumption on Precision-Recall Curves.” In *2010 20th International Conference on Pattern Recognition*, 4263–66. IEEE.
- Davis, Jesse, and Mark Goadrich. 2006. “The Relationship Between Precision-Recall and ROC Curves.” In *Proceedings of the 23rd International Conference on Machine Learning*, 233–40.
- Dietterich, Thomas G. 1998. “Approximate Statistical Tests for Comparing Supervised Classification Learning Algorithms.” *Neural Computation* 10 (7): 1895–1923.
- Fawcett, Tom. 2006. “An Introduction to ROC Analysis.” *Pattern Recognition Letters* 27 (8): 861–74.
- Flach, Peter, and Meelis Kull. 2015. “Precision-Recall-Gain Curves: PR Analysis Done Right.” *Advances in Neural Information Processing Systems* 28.
- Grau, Jan, Ivo Grosse, and Jens Keilwagen. 2015. “PRROC: Computing and Visualizing Precision-Recall and Receiver Operating Characteristic Curves in r.” *Bioinformatics* 31 (15): 2595–97.
- Green, David Marvin, and John A Swets. 1966. *Signal Detection Theory and Psychophysics*. Vol. 1. Wiley New York.
- Hanley, James A, and Barbara J McNeil. 1982. “The Meaning and Use of the Area Under a Receiver Operating Characteristic (ROC) Curve.” *Radiology* 143 (1): 29–36.
- Marzban, Caren. 2004. “The ROC Curve and the Area Under It as Performance Measures.” *Weather and Forecasting* 19 (6): 1106–14.
- Mazzanti, Samuele. 2020. “Why You Should Stop Using the ROC Curve: The Most Popular Metric May Not Be as Meaningful as You Think.” 2020. <https://towardsdatascience.com/why-you-should-stop-using-the-roc-curve-a46a9adc728>.
- Raschka, Sebastian. 2018. “Model Evaluation, Model Selection, and Algorithm Selection in Machine Learning.” *arXiv Preprint arXiv:1811.12808*.
- Roser, Max, Cameron Appel, and Hannah Ritchie. 2013. “Human Height.” *Our World in Data*.
- Saito, Takaya, and Marc Rehmsmeier. 2015. “The Precision-Recall Plot Is More Informative Than the ROC Plot When Evaluating Binary Classifiers on Imbalanced Datasets.” *PloS One* 10 (3): e0118432.
- Stevens, Stanley Smith. 1946. “On the Theory of Scales of Measurement.” *Science* 103 (2684): 677–80.
- Vabalas, Andrius, Emma Gowen, Ellen Poliakoff, and Alexander J Casson. 2019. “Machine Learning Algorithm Validation with a Limited Sample Size.” *PloS One* 14 (11): e0224365.
- Wixted, John T. 2020. “The Forgotten History of Signal Detection Theory.” *Journal of Experimental Psychology: Learning, Memory, and Cognition* 46 (2): 201.
- Zhou, Tao. 2023. “Discriminating Abilities of Threshold-Free Evaluation Metrics in Link Prediction.” *Physica A: Statistical Mechanics and Its Applications*, 128529.

## Appendix

### A. Linear approximation method for resolving power

The resolving power approach from the main text has a couple of disadvantages: It requires estimating the response curves over many grid points and choosing a specific  $\alpha$  value for the confidence interval width. This section outlines a local, linear approximation that avoids both of those drawbacks. Return to the toy example from Section 4, where we wish to compare the resolving power of the AUSGC versus the AUROC. The linear approach is easier to express by flipping the axes, plotting the AUSGC on the x-axis and the AUROC on the y-axis, as shown in Figure 8.

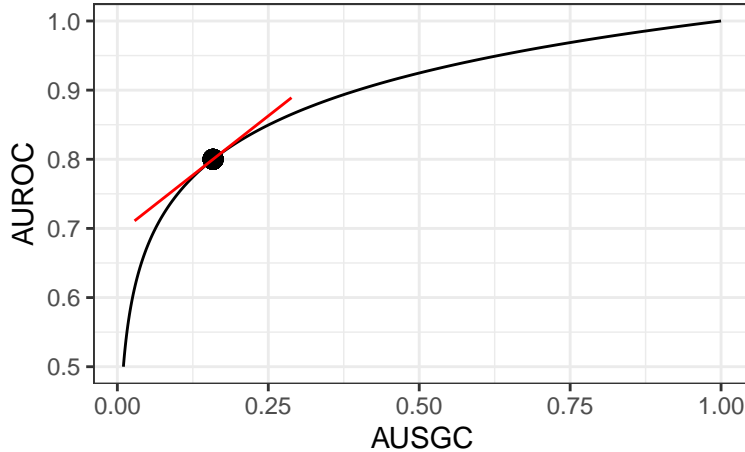


Figure 8: Response curve plotting the AUROC references scale on the y-axis. A linear approximation of the response function at the evaluation point is shown in red.

Suppose we want to compare the resolving power of the AUSGC versus the AUROC at the point (0.16, 0.8) shown in black. Figure 8 shows the full response curve, but we only need to evaluate a few points to estimate the tangent line shown in red. The slope at the evaluation point, which gives the relative signal of the two metrics, is 0.69. Since the slope is less than 1 it means the AUSGC has a relatively stronger response to improvements in model quality.

Next, we must estimate sampling variability at the evaluation point. Again, suppose we form many simulation samples of the evaluation metrics. But instead of finding percentile confidence intervals, we use the simulation samples to estimate the standard deviation of the AUSGC and AUROC, denoted respectively as  $\hat{\sigma}_S$  and  $\hat{\sigma}_R$ . If we assume that the distribution of the sample AUROC is approximately normal, then we can form a  $1 - \alpha$  confidence interval by selecting a  $z_{(1-\alpha/2)}$  critical value and multiplying the standard error. Using  $z_{(1-\alpha/2)} = 1.96 \approx 2$  gives an approximate 95 percent confidence interval. So for the AUROC we get the interval:  $[-2\hat{\sigma}_R, 2\hat{\sigma}_R]$ . The metric resolution (the width of the confidence interval in AUROC units) is then  $\kappa_{ROC} = 4\hat{\sigma}_R$ . Similarly, the approximate 95 percent confidence interval for the AUSGC is  $[-2\hat{\sigma}_S, 2\hat{\sigma}_S]$ . Now we use the linear approximation to map AUSGC to the AUROC scale. Suppose the slope of the linear approximation is  $\beta_1$  and the intercept is  $\beta_0$ , then we obtain the confidence interval  $[-2\hat{\sigma}_S\beta_1 + \beta_0, 2\hat{\sigma}_S\beta_1 + \beta_0]$  and its width is  $\kappa_{SGC} = 4\hat{\sigma}_S\beta_1$ . Taking the ratio of metric resolutions gives:

$$\frac{\kappa_{SGC}}{\kappa_{ROC}} = \frac{4\hat{\sigma}_S\beta_1}{4\hat{\sigma}_R} = \frac{\beta_1\hat{\sigma}_S}{\hat{\sigma}_R}$$

The  $z$  critical value cancels and we are left with the ratio of standard errors scaled in AUROC units. Thus, the linear approach requires only comparing the ratio of the standard errors to the slope of the response curve, eliminating the need for an  $\alpha$  level. Using the Leibniz notation  $\beta_1 = \frac{dR}{dS}$ , we must only check the inequality:

$$\frac{dR}{dS} > \frac{\hat{\sigma}_R}{\hat{\sigma}_S} \quad (\text{A.1})$$

Inequality A.1 makes transparent the signal to noise comparison. The left side of the inequality is the relative signal of the two metrics while the right side is the relative noise. If the inequality holds it means that the signal of the AUROC overwhelms its noise, giving it relatively greater resolving power.

The simplicity of the linear approach bears both its strengths and its weaknesses. Estimating the tangent curve requires only a few points in the immediate vicinity of the evaluation point, obviating the need to find the full response curve or choose a confidence interval width. The approach crucially assumes:

- i. The metric sampling distribution is symmetric.
- ii. A line is a good approximation of the response curve over the region of interest.

Recall that we calculate metric resolution by using the response curve to map confidence interval limits from one scale to another. A linear function will give a satisfactory approximation when these confidence limits are narrow, but it will be poor for wide confidence intervals bracketing a response curve segment that has a rapidly changing slope.

## B. Binormal results for different sample sizes

We extend the binormal investigation to sample sizes that are an order of magnitude smaller and larger than those presented in the main text. Beginning with  $N = 1000$ , the simulation was again repeated three times with estimates averaged across runs. Results are shown in Figure 9.

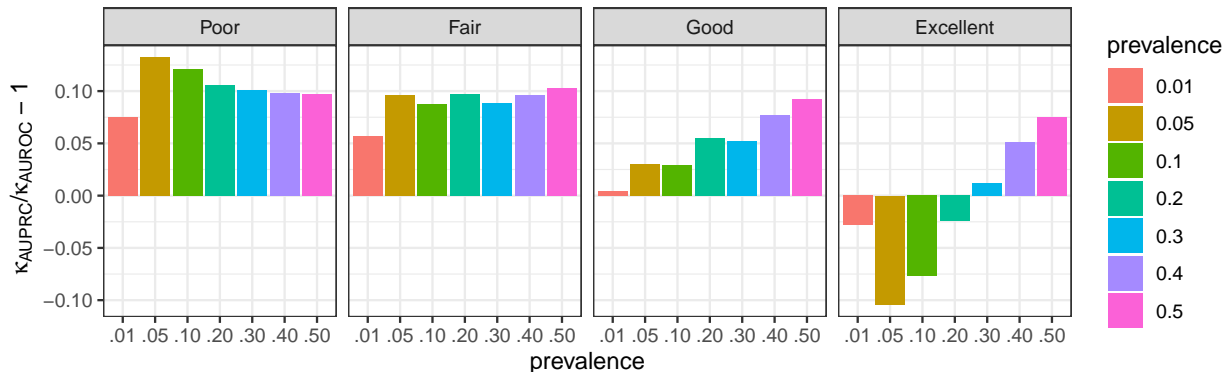


Figure 9: Relative resolution of AUPRC versus AUROC by outcome prevalence and model quality for a binormal model with a sample size of  $N = 1000$ . At each level of model quality 10,000 simulations are taken from the sampling model. Confidence limits are found from the .025 and .975 quantile values of the simulation samples.

Interestingly, the direction of the differences across conditions are the same as the  $N = 10,000$  scenario. Only the relative magnitudes have changed. Specifically, the AUPRC has superior resolving power only for “excellent” models with an outcome prevalence of 20 percent or less. The primary difference in magnitudes are found in the one percent prevalence condition, which now shows a smaller disadvantage for the fair to good models, and a smaller advantage for the excellent models. Note that for one percent prevalence there are now only ten instances in the positive class.

Finally, we repeat the study for an increased order of magnitude at  $N = 100,000$ . This simulation was only conducted once (not repeated and averaged like the previous two studies). Results are similar to the  $N = 10,000$  condition. There is one condition where the direction of the effect has flipped—the excellent model condition with a prevalence of 30 percent—though the relative difference is essentially zero. The other



primary difference is that the AUPRC is now at the biggest disadvantage for the one percent prevalence “fair” model condition.

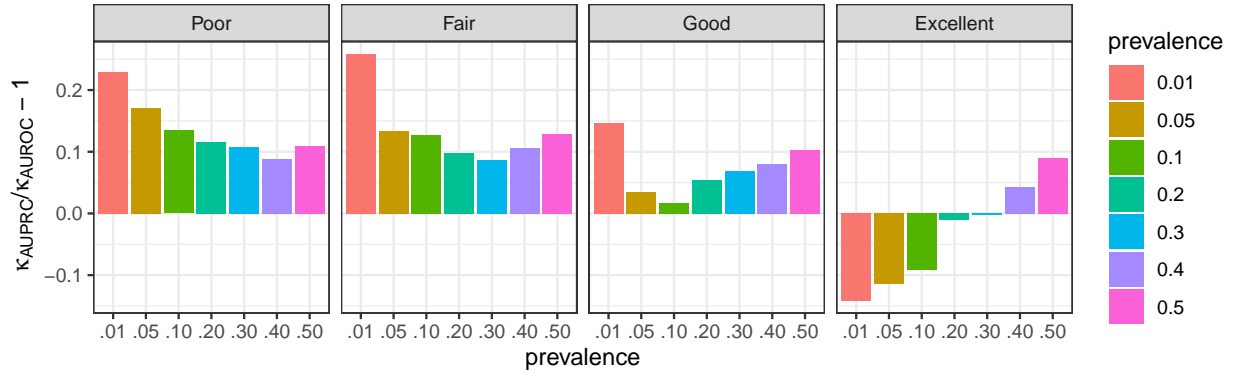


Figure 10: Relative metric resolution by outcome prevalence and model quality for a binormal model with a sample size of  $N = 100,000$ . At each level of model quality 10,000 simulations are taken from the sampling model. Confidence limits are found from the .025 and .975 quantile values of the simulation samples.

In summary, differences in sample size for the binormal model generally do not affect the direction of the effects, only their relative size. The AUPRC maintains its advantage only for excellent ( $\text{AUROC} = 0.95$ ) models with an outcome prevalence of 20 percent or less.